ELSEVIER

Chemical Geology 186 (2002) 301–313

CHEMICAL GEOLOGY
INCLUDING
ISOTOPE GEOSCIENCE

www.elsevier.com/locate/chemgeo

Comparative characterization of volcanic ash soils exposed to decade-long elevated carbon dioxide concentrations at Mammoth Mountain, California

Jennie C. Stephens, Janet G. Hering*

Environmental Engineering Science Department, California Institute of Technology, MC 138-78, Pasadena, CA 91125, USA

Accepted 18 January 2002

Abstract

Elevated concentrations of soil CO_2, ranging from 20% to 90%, from a magmatic source have been killing coniferous trees in the last decade in several distinct areas on the flanks of Mammoth Mountain, California. These areas of elevated soil CO_2 provide a natural laboratory to examine how chemical weathering in soils responds to extremely high-CO_2 concentrations in conjunction with possible changes in organic acids resulting from vegetation mortality. These volcanic ash soils have a particularly low resistance to chemical weathering due to the predominance of volcanic glass and other noncrystalline phases. Thus, decade-long exposure to anomalous conditions may result in differences in soil characteristics. Soil samples from within the high-CO_2 region have been analyzed and compared to samples from outside the anomalous area in the adjacent healthy forest areas where background CO_2 concentrations are less than 1%. Compared to the control soil, the high-CO_2 soil has lower pH values (5.0 compared to 5.6), higher soil moisture content, and higher surface area. Dithionite-citrate and acid-oxalate extractants were less effective in leaching Al and Si from the high CO_2 than from the control soil, indicating a distinct difference in the mineralogy of these soils. The observed differences between the high-CO_2 and control soils are consistent with an enhancement of weathering intensity in the soil exposed to elevated CO_2 concentrations.

Keywords: Mineral weathering; Organic acids; Mineralogy; Selective extractions

1. Introduction

Elevated concentrations of soil CO_2 derived from the venting of magmatic CO_2 have caused the death of coniferous trees in several distinct areas on Mammoth Mountain, California (Farrar et al., 1995; Hill, 1996; McGee and Gerlach, 1998; Rahn et al., 1996; Rogie et al., 2001). The initiation of CO_2 degassing has been attributed to a swarm of small earthquakes in 1989 (Gerlach et al., 1998; Hill et al., 1990); tree mortality in this area was first observed in 1990 (Farrar et al., 1995). High concentrations of soil CO_2 can cause tree mortality either by preventing the tree roots from absorbing O_2 needed for respiration or by interfering with nutrient uptake (Sorey et al., 1996). Surveys of soil gas in the upper 70 cm of the soil have documented CO_2 concentrations ranging from 20% to 90% within the tree-kill areas (Fig. 1b). The concentrations

* Corresponding author. Tel.: +1-626-395-3644; fax: +1-626-395-2940.

E-mail addresses: jennie@its.caltech.edu (J.C. Stephens), jhering@its.caltech.edu (J.G. Hering).

0009-2541/02/$ - see front matter
PII: S0009-2541(02)00007-4

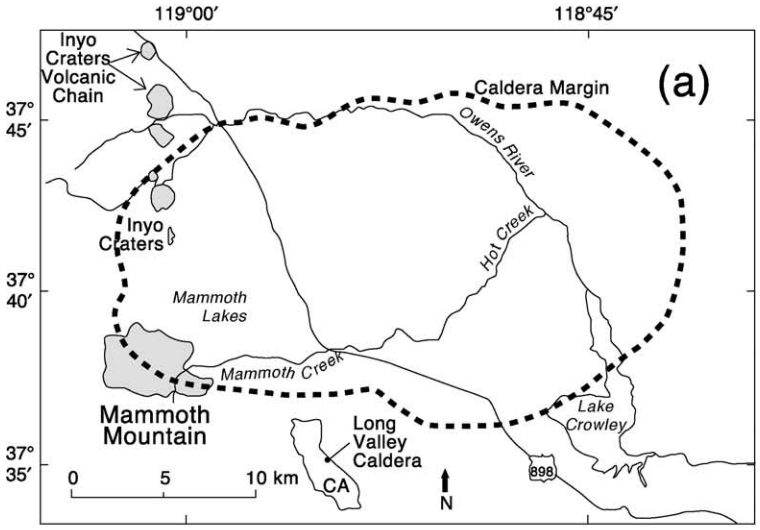
119°00′
118°45′
Inyo Craters Volcanic Chain
Caldera Margin
(a)
37° 45′
Owens River
Hot Creek
Inyo Craters
37° 40′
Mammoth Lakes
Mammoth Creek
Lake Crowley
Mammoth Mountain
Long Valley Caldera
37° 35′
0 5 10 km
CA
N
898

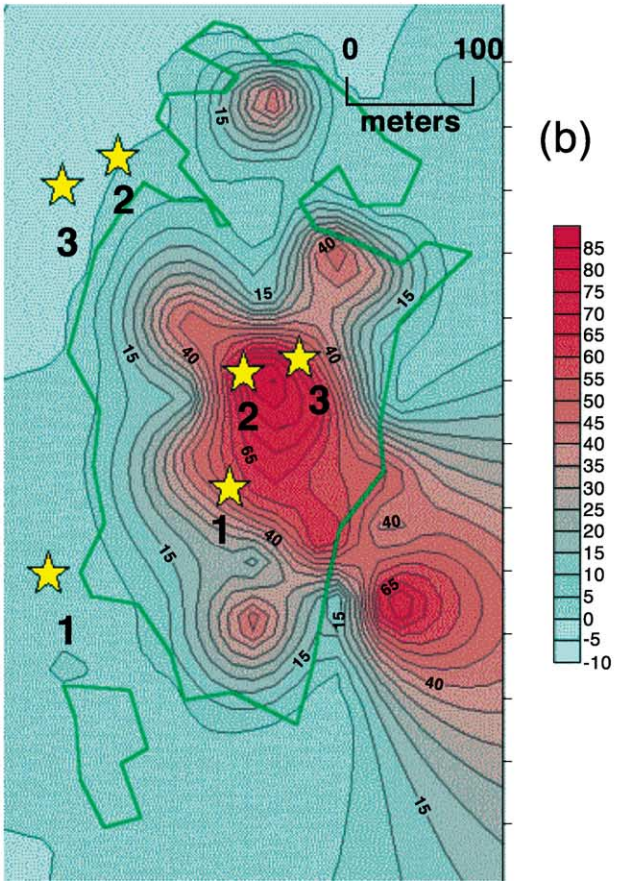
0 100
meters
(b)
85
80
75
70
65
60
55
50
45
40
35
30
25
20
15
10
5
0
-5
-10
1
2
3

of CO_2 in the adjacent healthy forest areas are at background levels of < 1% (Farrar et al., 1995; McGee and Gerlach, 1998; Rogie et al., 2001). Soil CO_2 concentrations vary seasonally with accumulation in the winter underneath the snowpack and a sudden decrease during spring snowmelt (McGee and Gerlach, 1998).

The tree-kill areas provide a natural laboratory to examine the response of soil mineral weathering to elevated CO_2 concentrations in conjunction with possible changes in organic acid composition resulting from vegetation mortality. Increased soil CO_2 concentrations cause a decrease in the pH of the soil solution and thus may (indirectly) increase weathering rates. Whether or not CO_2 itself has a direct effect on mineral weathering is not well understood. Some low-molecular-weight (LMW) organic acids produced in soils have been shown to accelerate mineral weathering (Drever and Stillings, 1997; Drever and Vance, 1994; Fox and Comerford, 1990; Gwiazda and Broecker, 1994).

The volcanic ash soils found at Mammoth Mountain have a particularly low resistance to chemical weathering due to the predominance of volcanic glass and other noncrystalline phases (Dahlgren et al., 1993). Decadal exposure of volcanic tephra to natural weathering conditions was found to produce distinct differences in the solid phases present in the weathered (as compared with the parent) material (Dahlgren et al., 1997). Thus, it may be anticipated that the decade-long exposure of the young volcanic soil at Mammoth Mountain to elevated soil CO_2 concentration may result in differences in soil characteristics.

Recent research on the Mammoth Mountain high-CO_2 areas has focused primarily on monitoring and characterizing the CO_2 fluxes and their relationship to seismic activity in the region (Farrar et al., 1995,1999; Gerlach et al., 1998; Hill, 1996; McGee and Gerlach, 1998; Rahn et al., 1996; Rogie et al., 2001; Sorey et al., 1996,1998). One study assessed the response of vegetation to the CO_2 degassing (Biondi and Fessenden, 1999) and another discussed possible effects of changing soil acidity on mobilization of aluminum (McGee and Gerlach, 1998). To date, however, the soil mineralogy and soil chemistry of this unique site have not been characterized. This paper presents a comparison of the soil chemistry and mineralogy and LMW organic acid composition in soils from a high-CO_2 and an adjacent control area.

2. Background

2.1. The field site

The soils analyzed for this study were sampled within and outside the Horseshoe Lake tree-kill, high-CO_2 area on Mammoth Mountain, located along the southwestern edge of the Long Valley caldera (Fig. 1a). The Horseshoe Lake tree-kill area occupies ~ 145,000 m^2 on 15–60% slopes at elevations of 2700–2800 m (McGee and Gerlach, 1998). The vegetation in the area is dominated by lodgepole pine (Biondi and Fessenden, 1999). Winter snowpack commonly exceeds 3 m but the soils remain unfrozen due to the insulating effect of the snowpack (McGee and Gerlach, 1998), and water infiltrates readily into the soil (Seney and Gallegos, 1995).

Although the geological parent material consists largely of granitic rock, the upper meters of the soil are derived from volcanic ash from the Inyo eruption, 650–550 years ago (Miller, 1985; Sieh, 2000). Volcanic ash soils are distinguished by a high percentage of noncrystalline volcanic glass and unique clay-size mineral assemblages often dominated by noncrystalline components (Dahlgren et al., 1993). Metastable solid phases with short-range order, including allophane, imogolite, and ferrihydrite are often formed as weathering products of volcanic glasses because of their rapid weathering rates (Dahlgren et al., 1993). Because of the comparatively rapid time-scale for weathering of volcanic ash soils (Dahlgren et al.,

Fig. 1. (a) Map showing location of study area, Mammoth Mountain, California and its relation to the Long Valley caldera (courtesy of USGS). (b) Map of Horseshoe Lake High-CO_2, tree-kill area and surroundings (courtesy of Dave Parker, UC Riverside). Sampling sites within and outside the anomalous area are marked with a star. The exact locations of sampling locations are high-CO_2 site 1: N 37°36′ 46.3 W 119°01′ 16.7; control site 1: N 37°36′ 46.5 W 119°01′ 23.6; high-CO_2 site 2: N 37°36′ 47.6 W 119°01′ 13.2; control site 2: N 37°36′ 46.4 W 119°01′ 05.2; high-CO_2 site 3: N 37°36′ 49.8 W 119°01′ 12.0; control site 3: N 37°36′ 46.1 W 119°01′ 04.6.

1993), the Mammoth Mountain soils may respond rapidly to changes in weathering conditions. Seasonal variations in the weathering rates at Mammoth Mountain are expected in response to precipitation and hydrologic flow patterns with minimal weathering in the dry summer months, accelerating weathering in the late fall and winter as the soils become moist, and maximum weathering in the late spring during snowmelt (McGee and Gerlach, 1998).

2.2. Soil mineral weathering

Rates of chemical weathering in soils are determined in part by the composition and characteristics of soil minerals. Mineral reactivity is highly variable (Chadwick and Chorover, 2001) and dependent on crystallinity (Eggleton, 1986) and surface area (Morel and Hering, 1993; Sposito, 1984). The chemical composition of infiltrating solution and the hydrologic and temperature regime of the local environment also play a large role in determining the chemical weathering rates in a given soil (Sparks, 1989).

Mineral dissolution necessarily involves four general steps: (1) transport of reactive species (e.g., H^+, OH^-, ligands, etc.) from the bulk solution to the mineral surface, (2) interaction of these reactive species with the surface metal centers (which destabilizes the bonds between the surface metal centers and crystal lattice), (3) detachment of the metal ion from the surface, and (4) transport of the reaction products (i.e., the metal ions) from the surface to the bulk solution. In transport-controlled dissolution, the rate-limiting supply of reactants or removal of products generates a concentration gradient between the surface and bulk solution (Stumm, 1992). In surface-controlled dissolution, the detachment step is usually considered to be rate limiting. The rates of proton-promoted dissolution (R_H) and ligand-promoted dissolution (ΣR_L, where L includes both organic and inorganic ligands) are generally taken to contribute additively to the overall dissolution rate R_{diss} though some synergistic effects have been observed (Kraemer et al., 1998).

$$R_{diss} = R_H + \sum R_L$$

This expression holds for systems sufficiently undersaturated that the back reaction (i.e., precipitation with rate R_{pptn}) can be neglected. As saturation is approached, the observed (net) dissolution rate, R_{diss}^{net}, decreases such that

$$R_{diss}^{net} = R_{diss} - R_{pptn}$$

with $R_{diss}^{net} = 0$ at equilibrium (Kraemer and Hering, 1997). Thus, ligands can increase observed dissolution rates by direct interaction with the surface metal centers (i.e., contributing to R_L) or indirectly by lowering the pH (i.e., contributing to R_H) or by stabilizing the dissolved metal in solution (i.e., decreasing R_{pptn}) (Drever and Stillings, 1997).

Clearly, increased concentrations of CO_2 could influence observed dissolution rates indirectly by decreasing pH. A direct role for CO_2 in mineral weathering has been proposed but is still controversial. Weathering rates measured at high temperature (100–200 °C) and high pCO_2 (2–20 bar) have been shown to be proportional to $pCO_2^{0.3}$ (Lagache, 1965). This apparent fractional dependence on pCO_2 has been attributed either to adsorption of CO_2 (Sverdrup, 1990) or simply as a pH effect (apparently the initial pH of the experiments with CO_2 was lower) (Brady, 1991; Helgeson et al., 1984). Despite this uncertainty, this relationship has been assumed to hold for CO_2 values typical of soil environments in several geochemical models (Marshall et al., 1988; Sverdrup and Warfvinge, 1993; Volk, 1987). Several studies attempting to verify this relationship have shown that, at low pH, weathering is not directly affected by CO_2 concentration (Brady and Carroll, 1994; Grandstaff, 1977; Wogelius and Walther, 1991), whereas both decreases (Wogelius and Walther, 1991) and increases (Berg and Banwart, 2000; Osthols and Malmstrom, 1995) in dissolution rates have been observed with increased CO_2 at alkaline pH, in addition to observations of no effect (Knauss et al., 1993; Malmstrom et al., 1996).

Weathering rates determined in the laboratory for many minerals (Langmuir, 1997) and for some whole soils (Asolekar et al., 1991) are often much higher than field weathering rates estimated from watershed-scale element budgets (April et al., 1986; Velbel, 1989). One source of uncertainty in this comparison is the mineral surface area exposed to weathering in the field. However, lower field weathering rates may also reflect the influence of hydrologic conditions and a shift from surface-controlled dissolution (under laboratory conditions) to transport-controlled dissolution (Kolka et al., 1996; Schnoor, 1990).

3. Methods

3.1. Sampling

Samples were collected in September 1999 and June 2000 from a total of six sites (Fig. 1b), three within and three outside the Mammoth Mountain Horseshoe Lake high-CO_2 area (unless otherwise noted, the results presented here are from the samples collected in September 1999). The sites were carefully selected based on extensive USGS monitoring data of the soil CO_2 concentrations (Rogie, 2001; Rogie et al., 2001). The sites within the high-CO_2 area were selected in regions of vegetation mortality where measured soil CO_2 concentrations are > 20% throughout the year and the control sampling sites in regions of healthy vegetation with background levels (< 1%) of soil CO_2. Each of the three control sites was chosen to correspond to one of the three high-CO_2 sites (based on elevation, slope, and aspect) in an attempt to minimize differences other than the vegetation and CO_2 concentration. The high-CO_2 site 1 and control site 1 are 200 m apart at an elevation of 2780 m and are on a slope of 50% facing east. The high-CO_2 site 2 and control site 2 are 300 m apart at an elevation of 2710 m and a slope of 20% facing southeast. The high-CO_2 site 3 and control site 3 are 300 m apart at an elevation of 2700 m and are on relatively flat terrain.

As is characteristic of volcanic ash soils (Shoji et al., 1993), these soils have a distinct organic litter layer (0–5 cm), a dark-colored organic A-horizon (5–45 cm) — where, in most of the soil pits, two distinct organic rich horizons (5–15 and 15–45 cm) could be distinguished — and a yellowish-brown B-horizon with minimal visible organic material (45–60 cm). Samples were taken from each of these horizons and homogenized before analysis. With the exception of pH and soil moisture measurements, the results presented here are from analysis of B-horizon soils sampled from a depth ranging from 45 to 60 cm. Although more intense weathering would be expected in the surface horizons, this comparative study focused on the subsurface B-horizon in an attempt to minimize variability associated with the vegetation mortality in the surface horizons. Samples were stored in polypropylene bags and refrigerated until they were analyzed. Within 48 h of sampling, upon return to the lab, pH and soil moisture were measured on the fresh soil samples; the remainder of the samples were dried and sieved through a 2-mm sieve and subsequently used in all other analyses.

3.2. Chemical analyses

Soil pH was measured in aqueous suspensions (at a 1:2 (w/w) soil/water ratio) following a 20-min equilibration. Soil moisture percentage was determined gravimetrically by measuring the difference in weight of the field-moist fresh sample and the same sample dried in an oven at 60 °C for 48 h. Particle-size distribution was determined by the pipette method (Gee and Bauder, 1986). BET-N_2 surface areas of whole soils (< 2 mm) and the clay-size fraction (< 2 μm) were measured using a Gemini 2360 Surface Area Analyzer (Micromeritics Instrument, Norcross, GA). Elemental analysis was performed by Chemex Laboratories on whole soil samples (< 2 mm) and on sand-, silt- and clay-size-fractionated samples using X-ray fluorescence (XRF) spectrometry. Percent weight of major elements as oxides was determined based on comparison with a certified standard reference material (SY-4, Canadian Certified Reference Materials Proj-ect) and organic carbon was estimated based on weight loss on ignition at 1010 °C. Three selective dissolution analyses were performed on both the high-CO_2 and control soils. In the dithionite-citrate dissolution procedure, 0.5 g of soil sample was mixed with 25 ml of 0.68 M sodium citrate; 0.4 g of dithionite powder ($Na_2S_2O_4$) was added and the suspension was shaken overnight in an end-over-end shaker (Carter, 1993). For dissolution with acid ammonium oxalate, 0.25 g of soil sample was mixed vigorously with 0.2 M ammonium oxalate adjusted to pH 3 in the dark for 2 h (McKeague and Day, 1966). For the pyrophosphate dissolution, 0.3 g of soil sample was mixed with 30 ml of 0.1 M sodium-pyrophosphate and shaken overnight in an end-over-end shaker (Carter, 1993). After each of these extraction procedures, the solutions were centrifuged and the supernatant was filtered with a cellulose acetate 0.2-μm filter and analyzed for Al, Si, Fe, Ca and K by inductively coupled plasma mass spectroscopy (ICP-MS).

Low-molecular-weight (LMW) organic acids and total organic carbon (TOC) were measured in aqueous extracts from soils collected in June 2000. Soil samples were extracted with water in a 1:2 (w/w) ratio shaken on an end-over shaker overnight. The suspen-

sion was then centrifuged at 4400 rpm for 10 min; the supernatant was filtered through a 0.45-μm filter and this aqueous extract was frozen until analyzed. LMW organic acids were analyzed by ion chromatography using a Dionex IonPac AS11 4 mm analytical column (and corresponding guard column) with detection by conductivity. Each run lasted 25 min using an eluent of NaOH with a concentration gradient of 0.50–38 mM. Concentrations of LMW organic acids were determined based on comparison with standards. TOC in the soil extracts was determined by high temperature catalytic oxidation using a Shimadzu TOC-5000A Total Organic Carbon Analyzer. The percentage of TOC accounted for by the measured concentrations of LMW organic acids was calculated.

Replicate analyses with different subsamples of soil were performed for all methods to assess the reproducibility of each method and the level of heterogeneity within each homogenized soil sample.

3.3. Mineralogical analyses

Thin sections of the bulk (<2 mm) size fraction soil were prepared and examined under a petrographic microscope. A minimum of 400 points of a grid on each slide was counted. Powder X-ray diffraction (XRD) analysis was performed on whole soil samples and clay-size fraction samples using a Scintag Pad V X-ray Powder Diffractometer using Cu K-α radiation generated with a 40-kV accelerating potential and 35-mA tube current. Samples were step scanned for 2 s at a rate of 0.01°/min at a 0.01° 2θ step. Diffractograms were obtained for samples treated with the following standard methods, including Mg and K saturation, glycolation, and heating to 550 °C (Whittig and Allardice, 1986). A Philips EM430 TEM at an accelerating voltage of 300 kV was used to examine samples of the <2-μm fraction for the presence of allophane, imogolite or ferrihydrite. Magnetite was separated from the bulk sample by using a magnet.

4. Results and discussion

4.1. pH measurements

The measured pH was approximately 5.0 in the high-CO_2 soil and approximately 5.6 in the control soil (Fig. 2). The pH was lower in the surface horizons than at depth, probably due to the higher concentration of soluble organic acids closer to the surface (Zabowski and Sletten, 1991). Since the ambient soil CO_2 concentrations are not maintained during sample collection and analysis, it is reasonable that the pH measured in the high-CO_2 soil is higher than the pH of 3.9–4.15 predicted for soil solution calculated based on CO_2 concentration data (McGee and Gerlach, 1998). The measured pH is similar to that of water (pH 5.3) from a well in the high-CO_2 area and lower than that of water (pH 7.0) from a nearby well outside the high-CO_2 area (Farrar et al., 1999).

4.2. Percent soil moisture

Although no distinct difference was observed in the moisture content of the high-CO_2 and control soils in the samples collected in early June during the snowmelt (Fig. 3a), the high-CO_2 soil was moister than the control soil in the samples collected in September, at the end of the summer (Fig. 3b). This difference in soil moisture content of the September samples probably reflects the absence of evapotranspiration by live trees throughout the dry summer months in the high-CO_2 soil.

4.3. Particle-size distribution

The Mammoth Mountain B-horizon soils have a low clay content of less than 2% by weight, while the

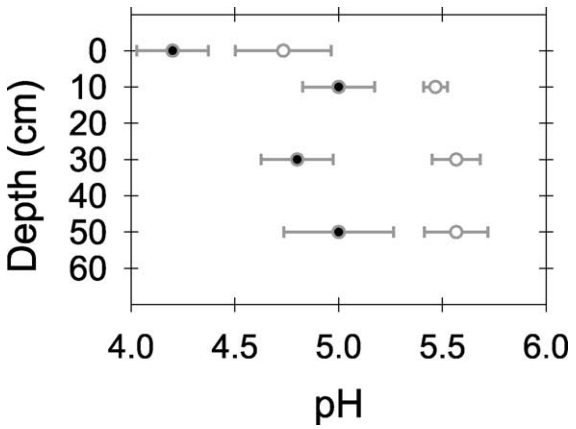

Fig. 2. Measurements of pH — Average and standard deviation of samples within the high-CO_2 soil (solid circles) and in the control soil (open circles) collected in September, 1999.

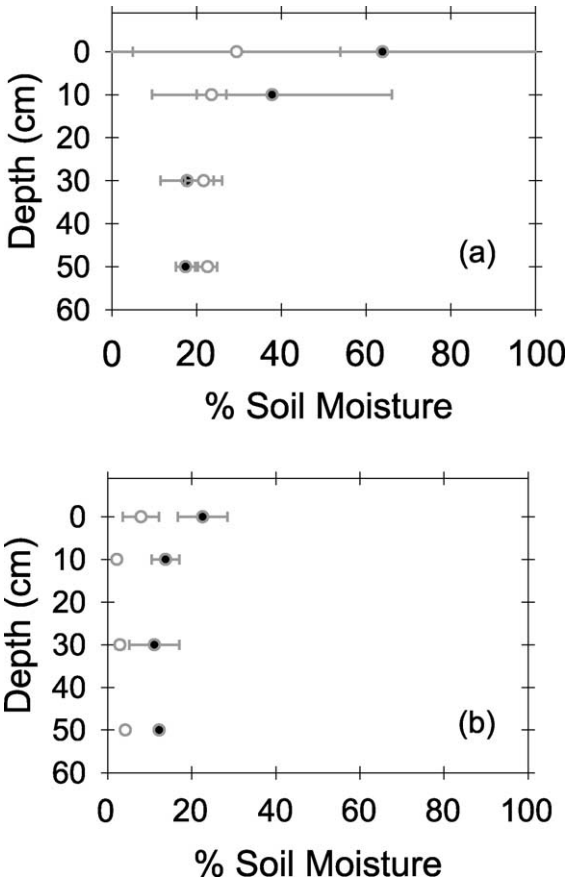

Fig. 3. Percent soil moisture — average and standard deviation of samples within the high-CO_2 soil (solid circles) and the control soil (open circles) collected in (a) June 2000, and (b) September 1999. Percent soil moisture = 100 × ((fresh weight − dry weight)/dry weight).

sand and silt-size particles make up 75–80% and 18–26% of the soil, respectively. Comparison with the results of a simultaneous analysis of a standard soil with a known particle-size distribution indicates that the range of values for sand and silt reflects the variations among the different sampling sites rather than error in the method. Rates of chemical weathering in volcanic ash soils are often estimated from the quantity of clay formed (Dahlgren et al., 1993). However, since the clay content of soils from both the high-CO_2 and control soils is comparable to the error of the method (± 1%) (Gee and Bauder, 1986), no comparison can be made between the sites.

4.4. Surface area

Surface areas measured in both whole soil samples (Fig. 4a) and clay-size fractions (Fig. 4b) are greater in the high-CO_2 soil than in the control soil. Replicate measurements on soil samples from each site were consistent (as shown by the error bars in Fig. 4). Thus, the differences among the high-CO_2 and control sites can be attributed to heterogeneity of the soil. Soil surface areas as measured by the BET-N_2 technique generally increase with soil age because the weathering process alters the mineral surface and breaks down soil particles (White, 1995). Thus, the higher surface area of the soil from the high-CO_2 sites suggests that they have experienced more intense weathering than the soil from the control sites with lower surface area.

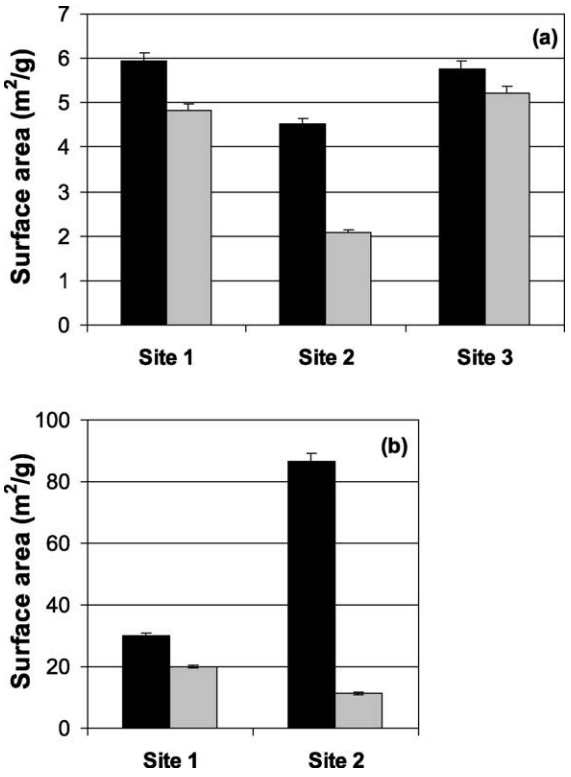

Fig. 4. Surface area measurements in B-horizon soils collected in September 1999. Average and standard deviation of replicate measurements (a) whole soil samples, (b) clay-size fraction. An insufficient quantity of the clay fraction from site 3 precluded analysis. Black = high-CO_2 soil. Grey = control soil.

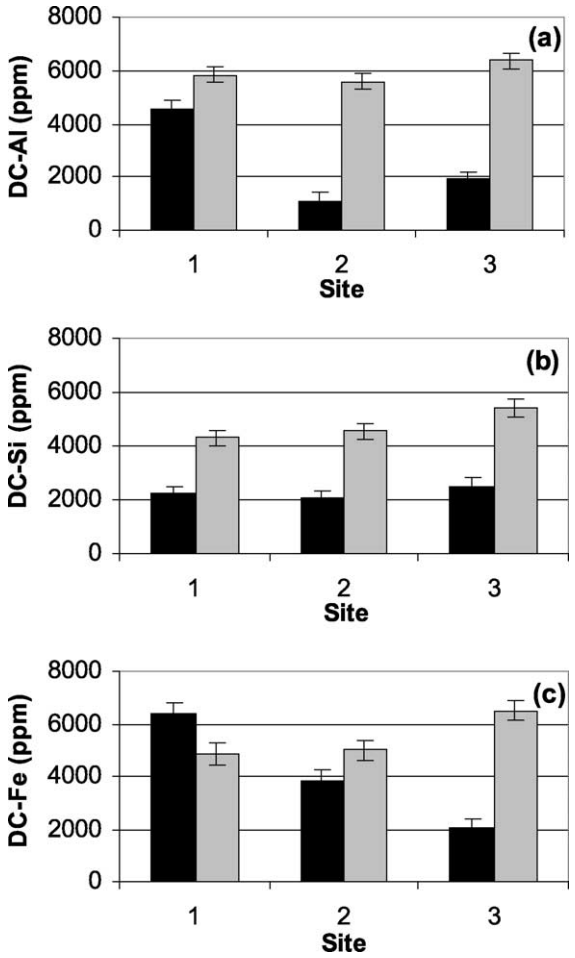

Fig. 5. Selective dissolution results from B-horizon soil collected in September 1999. Dithionite-citrate extractable (a) Al (DC–Al), (b) Si (DC–Si), (c) Fe (DC–Fe). Error bars represent range of duplicate samples. Black = high-CO_2 soil. Grey = control soil.

4.5. Mineralogical analysis

Bulk mineralogy of the soil was evaluated by XRD and visual examination using a petrographic microscope. The soils are predominantly composed of volcanic glass (50–60%). Plagioclase and K-feldspars, quartz, hornblende, magnetite, and cristobolite occur as accessory minerals. Halloysite, kaolinite, and vermiculite were identified by XRD in the clay-size fraction. Ferrihydrite was identified by TEM analysis of the clay-size fraction but neither allophane or imogolite was detected. Low intensities and poor signal/noise ratios were observed in the X-ray diffractograms of these samples consistent with the high percentage of noncrystalline material in these soils (Stephens, 2002, in preparation). Thus, although distinct clay minerals were identified, any quantitative differences between the clay mineralogy of the high-CO_2 and control soils that may have resulted from 10 years of different weathering conditions were too subtle to be observed.

4.6. Elemental analysis

Analysis of the major elemental composition of the soils is shown in Table 1. Compared to the control samples, the high-CO_2 soil is slightly enriched in Si and depleted in Al. This pattern suggests that Al may have been preferentially weathered from the high-CO_2 soils either because the high-CO_2 soils were subject to more intense weathering or because less organic matter is available to bind Al in the high-CO_2 soil (see Section 4.8). The other major elements do not show any consistent differences between the high-CO_2 and control soils. Variability in the other major elements indicates a high degree of spatial heterogeneity in the bulk mineralogy. As was found in another decade-long study of weathering of volcanic material (Dahlgren et al., 1997), total elemental analysis may not be a sufficiently sensitive technique to identify distinct differences in weathering in short-term studies.

4.7. Selective extractions

Three selective dissolution analyses were performed using dithionite-citrate, ammonium oxalate, and sodium-pyrophosphate as extractants. The results shown in Figs. 5 and 6 indicate differences in soil mineralogy between the high-CO_2 and control sites.

Table 1
Major elemental chemistry of the inorganic fraction of the bulk (<2 mm) soil (in wt.%); all other elements are less than 1%

		SiO_2	Al_2O_3	K_2O	Na_2O	Fe_2O_3	CaO
High CO_2	1	72.7	14.3	4.4	3.5	2.8	1.2
	2	73.4	13.8	4.8	3.4	2.3	1.0
	3	73.7	13.3	5.0	3.6	1.7	0.9
Control	1	72.4	14.5	4.5	3.5	2.3	1.0
	2	70.6	15.1	4.2	3.7	2.7	1.4
	3	69.2	16.8	3.9	3.9	3.0	1.7
Precision[a]		± 0.3	± 0.4	± 0.05	± 0.2	± 0.3	± 0.03

[a] Based on replicate analyses.

4.7.1. Dithionite-citrate extraction

In the dithionite-citrate extractions, the quantities of extractable Al and Si (DC–Al and DC–Si) are consistently lower in the high-CO_2 soil compared to the control soil (Fig. 5a,b). No consistent pattern was observed for iron extracted by dithionite-citrate (DC–Fe) (Fig. 5c). The dithionite-citrate extraction is generally assumed to dissolve crystalline oxide phases, noncrystalline phases and organically complexed Al and Fe (Mehra and Jackson, 1960). Approximately 1.5–8.5% of Al, 0.6–1.3% of Si, and 14–46% of Fe were leached from these soils in this extraction.

4.7.2. Acid-oxalate extraction

The results of the acid ammonium oxalate dissolution show trends similar to the dithionite-citrate results for Al (AO–Al), Si (AO–Si) and Fe (AO–Fe). More AO–Al and AO–Si are extracted from the control soil than from the high-CO_2 soil from each site while AO–Fe varies considerably (Fig. 6a–c). The oxalate extraction dissolved < 1.5% of Si, up to 7% of Al, and a highly variable 2–26% of Fe. Acid ammonium oxalate extraction of soils has been shown to dissolve noncrystalline materials selectively (Fey and Roux, 1977), although it may also partially dissolve magnetite (Baril and Bitton, 1969) and some layer silicates (Carter, 1993).

4.7.3. Pyrophosphate extraction

The results of the Na-pyrophosphate dissolution show considerable variability in the quantities of Fe (P_2O_5–Fe) and Al (P_2O_5–Al) extracted (Fig. 6d,e). Unlike the other dissolution methods, no clear trend is apparent in the comparison of the high-CO_2 and control soils. Na-pyrophosphate, which extracts organically bound Fe and Al, dissolved < 1.5% of total Al and only up to 7% of total Fe, suggesting that organically complexed metals are not a major soil component.

4.7.4. Interpretation and critique of results of selective extractions

A distinct difference in the mineralogy of the high-CO_2 soil compared to the control soil is indicated by

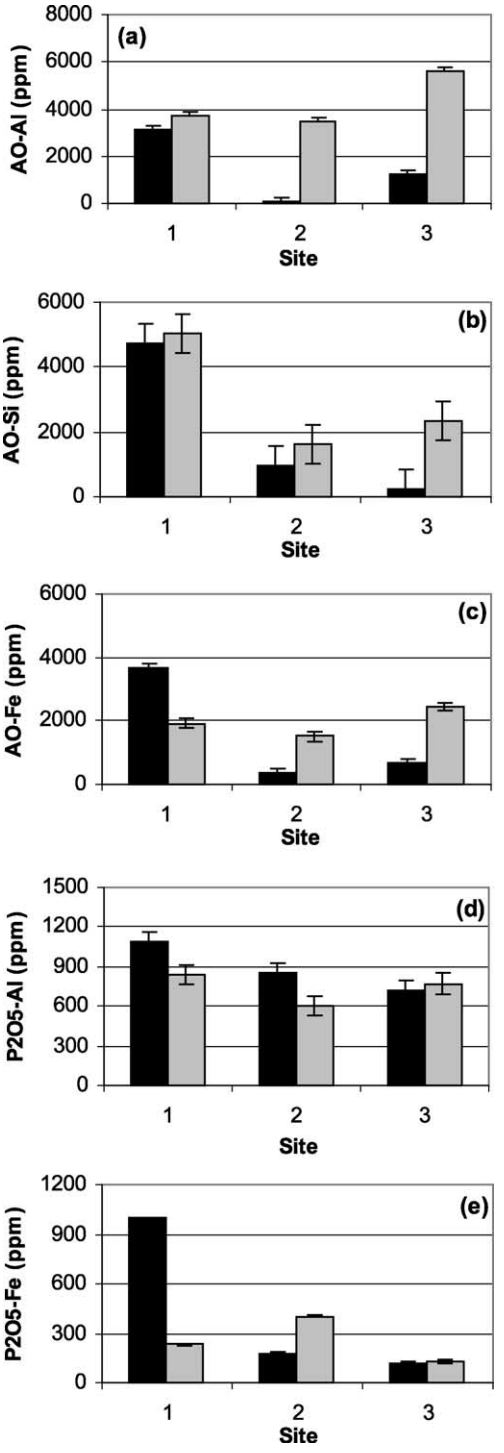

Fig. 6. Selective dissolution results from B-horizon soil collected in September 1999. Acid ammonium oxalate extractable (a) Al (AO–Al), (b) Si (AO–Si), and (c) Fe (AO–Fe), and sodium-pyrophosphate extractable (d) Al (P_2O_5–Al) and (e) Fe (P_2O_5–Fe). Error bars represent standard deviation of at least three replicate samples. Black = high-CO_2 soil. Grey = control soil.

differences in the efficiencies of the dithionite-citrate and acid-oxalate extraction for these soils. Although assignment of extractable metal concentrations to specific mineral phases can be unreliable (McCarty et al., 1998), we suggest that the observed patterns can be related to the weathering history of the soils. The extraction of less Al and Si by both extractants is, however, subject to different possible interpretations. This observation could be taken to indicate that the high-CO_2 soil has been subject to greater weathering intensity and thus more of the mineral phases extractable by dithionite-citrate and acid-oxalate had been weathered out of the high-CO_2 soil compared to the control soil. Alternatively, if the dithionite-citrate and acid-oxalate extractable fractions are taken to correspond to weathering products, this observation could reflect less intensive weathering (i.e. less formation of weathering products) in the high-CO_2 soil. However, the Mammoth Mountain soils have been weathering for hundreds of years and thus the weathering products accumulated over the last 10 years during the period of CO_2 degassing would be insignificant relative to the total accumulation of weathering products. Therefore, we suggest that the difference in extractable material between the high-CO_2 and control soils reflects more intense weathering in the high-CO_2 soil.

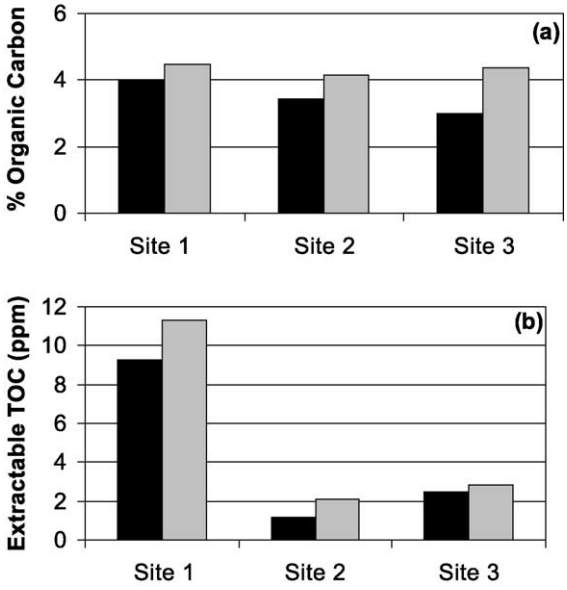

Fig. 7. (a) Total organic carbon percent by weight. (b) Total organic carbon (TOC) in aqueous extracts of 1:2 (w/w) soil/water. Units of part per million (ppm) represent milligrams of organic carbon per kilogram of soil extract. Black = high-CO_2 soil. Grey = control soil.

4.8. Organic analysis

4.8.1. Total organic carbon

Organic carbon in these B-horizon soils makes up 3–5% of the total soil material, and there is less organic material in the high-CO_2 soil than in the control soil (Fig. 7a). Vegetation mortality in the high-CO_2 soil has halted the normal deposition of litter as well as the input of organic acids from roots. These effects might be even more pronounced in the upper soil horizons; the subsurface B-horizon was chosen for this comparative study in an attempt to minimize differences in the organic fraction expected from the vegetation mortality.

4.8.2. Low-molecular-weight organic acids

Analysis of soil–water extracts by ion chromatography identified six primary organic acids present in the B-horizon soils: acetic, oxalic, citric, propionic, formic and malic (Table 2). Acetic acid is most abundant ranging from 40 to 100 μmol/kg, followed by formic, propionic, oxalic, citric, and malic acid with less than 3 μmol/kg. Concentrations of oxalic acid, which has been widely demonstrated to enhance mineral weathering (Drever and Stillings, 1997), range from 3 to 6 μmol/kg, consistent with measurements in other soils (Fox and Comerford, 1990). No clear or significant trends are observed in the comparison of the organic acid concentrations in the high-CO_2 and control soils.

The measured concentrations of LMW organic acids reflect a complex and dynamic balance between organic acid production and decomposition. LMW organic acids are produced primarily at plant roots and also by decomposition of organic matter (Drever and Vance, 1994; Pohlman and McColl, 1988), so their concentrations may be dependent on micro-scale proximity to plant biomass. Seasonal variation in LMW organic acid concentrations is also likely, as organic acids can be removed by flushing during the spring snowmelt. Since our analysis of LMW organic acids was performed on soil samples collected in June just after the snowmelt, the organic acid concentrations and their relative abundance in the high-CO_2 and control soils may not be entirely representative. The similar abundance of LMW organic acids in the high-CO_2 and

Table 2
Concentrations of LMW organic acids determined by ion chromatography (μmol/kg)

	High-CO_2 sites			Control sites		
	1	2	3	1	2	3
Acetic	102.2	52.6	68.3	98.7	41.8	61.0
Formic	29.2	14.0	21.3	33.4	13.8	17.2
Propionic	21.1	22.8	27.8	21.3	9.6	16.2
Oxalic	6.1	3.6	4.5	5.3	3.1	3.7
Citric	2.4	0.8	0.5	4.9	ND[a]	1.6
Malic	2.8	1.7	1.7	1.6	0.8	1.4
Percent of TOC[b]	1.9	8.6	5.1	2.1	4.2	3.6

[a] Not detected.
[b] Percent of extractable TOC accounted for by the sum of all measured LMW organic acids.

control soils suggests that these soil constituents do not contribute to the differences in weathering intensity experienced by these soils. However, a contribution of LMW organic acids to mineral weathering at these sites cannot necessarily be excluded because spatial and seasonal variations in LMW organic acid concentrations have not yet been examined.

4.8.3. Extractable total organic carbon and LMW organic acids

Total organic carbon (TOC) in the aqueous extracts is greater in the control soil than in the high-CO_2 soil (Fig. 7b), a result consistent with the vegetation mortality in the high-CO_2 soil and the higher percentage of organic matter measured in the control soil (Fig. 7a). The measured concentrations of LMW organic acid constitute only a small percentage of TOC, ranging from 2% to 9%, suggesting that the majority of extractable organic carbon in these soils is present as medium- to high-molecular-weight compounds, such as humic substances. Humic substances are thought to have only slight effects on mineral dissolution and both inhibition and acceleration of mineral weathering (depending on pH) have been observed (Hering, 1995; Ochs, 1996; Ochs et al., 1993).

4.9. Temperature effect

An alternate explanation for differences in the weathering intensity of the high-CO_2 soil compared to the control soil could be temperature, since a temperature dependence of weathering of volcanic ash soils has been identified (Dahlgren et al., 1993). The CO_2 gas diffusing through the soil at Mammoth Mountain, however, is at ambient temperatures (Farrar et al., 1999), so no temperature difference between the sites is expected.

5. Conclusions

The results of this comparative characterization demonstrate some distinct differences between the high-CO_2 and control soils. The high-CO_2 soil is exposed to elevated soil CO_2 concentrations, lower pH, and higher soil moisture content (during late summer). It also exhibits a slight depletion of total Al and enrichment of total Si, and lower concentrations of extractable Al and Si than the control soils. The observed differences are consistent with the hypothesis that the high-CO_2 soil has experienced more intense weathering resulting from either the higher CO_2 concentrations or the lower pH or both. This hypothesis is supported by the observation that the concentrations of Si, Al, Mn and Fe measured in well-water within the Horseshoe Lake high-CO_2 area are higher than those measured in nearby wells outside the anomalous area (Evans, 2001; Farrar et al., 1999).

Although we hypothesize that the high-CO_2 soil has experienced enhanced weathering, it is not possible to attribute this to direct effects of CO_2 on weathering rates (i.e., a contribution of R_L to R_{diss} where $L = CO_2$) because of the lower pH (which would tend to increase the rate of proton-promoted dissolution, R_H) and the potential changes in LMW organic acids due to vegetation mortality. Further work is needed to explain the observed differences between the high-CO_2 and control soils and to identify specific mechanisms by which altered weathering conditions (including elevated CO_2 concentrations, lower pH, and the vegetation mortality) determine weathering rates. Although concentrations of LMW organic acids measured in the high-CO_2 and control soils did not show any consistent trends, spatial and seasonal variations in organic acid concentrations need to be examined to determine whether organic acids might be contributing to enhanced weathering. In addition, laboratory soil dissolution experiments under controlled and varied CO_2 and organic acid concentrations may provide some insight into how elevated CO_2 concentrations at Mammoth Mountain affect the weathering of these volcanic ash soils.

Acknowledgements

We thank the reviewers, Oliver Chadwick and Paul Schroeder, for their comments and helpful criticisms which improved the manuscript. We thank Dr. Robert C. Graham of UC Riverside for his suggestions, Dr. Chi Ma for help in interpreting our XRD diffractograms, John Rogie for sharing his knowledge of the field site and Johnny Lam for his assistance with the analysis of organic acids. Financial support from the American Chemical Society Petroleum Research Fund (Grant # 34558-AC2), the ARCS Foundation, an EPA STAR Graduate Fellowship, and an NSF Graduate Fellowship is gratefully acknowledged.

References

April, R., Newton, R., Coles, L.T., 1986. Chemical weathering in two Adirondack watersheds: past and present-day rates. Geol. Soc. Am. Bull. 97, 1232–1238.

Asolekar, S.R., Valentine, R.L., Schnoor, J.L., 1991. Kinetics of chemical weathering in B horizon spodosol fraction. Water Resour. Res. 27 (4), 527–532.

Baril, R., Bitton, G., 1969. Teneurs élevées de fer libre et identification taxonnomique de certain sols due Québec contenant de la manetite. Can. J. Soil Sci. 52, 19–26.

Berg, A., Banwart, S.A., 2000. Carbon dioxide mediated dissolution of Ca-feldspar: implications for silicate weathering. Chem. Geol. 163 (1–4), 25–42.

Biondi, F., Fessenden, J.E., 1999. Response of lodgepole pine growth to CO_2 degassing at Mammoth Mountain, California. Ecology 80 (7), 2420–2426.

Brady, P.V., 1991. The effect of silicate weathering on global temperature and atmospheric CO_2. J. Geophys. Res. 96 (B11), 18101–18106.

Brady, P.V., Carroll, S.A., 1994. Direct effects of CO_2 and temperature on silicate weathering: possible implications for climate control. Geochim. Cosmochim. Acta 58 (8), 1853–1856.

Carter, M.R., 1993. Soil Sampling and Methods of Analysis Lewis Publishers, Boca Raton, FL.

Chadwick, O.A., Chorover, J., 2001. The chemistry of pedogenic thresholds. Geoderma 100, 321–353.

Dahlgren, R., Shoji, S., Nanzyo, M., 1993. Mineralogical characteristics of volcanic ash soils. In: Shoji, S., Dahlgren, R., Nanzyo, M. (Eds.), Volcanic Ash Soils, Genesis, Properties, and Utilization. Developments in Soil Science. Elsevier, Amsterdam.

Dahlgren, R., Dragoo, J., Ugolini, F., 1997. Weathering of Mt. St. Helens Tephra under a cryic-udic climate regime. Soil Sci. Soc. Am. J. 61, 1519–1525.

Drever, J.I., Stillings, L.L., 1997. The role of organic acids in mineral weathering. Colloids Surf., A 120, 167–181.

Drever, J.I., Vance, G.F., 1994. Role of soil organic acids in mineral weathering processes. In: Pittman, E.D., Lewan, M.D. (Eds.), Organic Acids in Geological Processes. Springer-Verlag, Berlin, pp. 138–161.

Eggleton, R.A., 1986. The relation between crystal structure and silicate weathering rates. In: Colman, S.M., Dethier, D.P. (Eds.), Rates of Chemical Weathering of Rocks and Minerals. Academic Press, Orlando, FL, pp. 21–40.

Evans, W.C., 2001. Personal communication. USGS, Menlo Park, CA.

Farrar, C.D., et al., 1995. Forest-killing diffuse CO_2 emission at Mammoth Mountain as a sign of magmatic unrest. Nature 376, 675–678.

Farrar, C.D., Neil, J.M., Howle, J.F., 1999. Magmatic Carbon Dioxide Emissions at Mammoth Mountain, California USGS, Sacramento, CA.

Fey, M.V., Roux, J.L., 1977. Properties and quantitative estimation of poorly crystalline components in sesquioxidic soil clays. Clays Clay Miner. 25, 285–294.

Fox, T.R., Comerford, N.B., 1990. Low-molecular weight organic acids in selected forest soils of the southeastern USA. Soil Sci Soc. Am. J. 54 (4), 1139–1144.

Gee, G.W., Bauder, J.W., 1986. Particle-size analysis. In: Klute, A. (Ed.), Methods of Soil Analysis: Part I, Physical and Mineralogical Methods. Soil Science Society of America, Madison, WI, pp. 383–413.

Gerlach, T.M., Doukas, M.P., McGee, K.A., Kessler, R., 1998. Three-year decline of magmatic CO2 emissions from soils of a Mammoth Mountain tree kill: Horseshoe Lake, CA, 1995–1997. Geophys. Res. Lett. 25 (11), 1947–1950.

Grandstaff, D.E., 1977. Some kinetics of bronzite orthopyroxene dissolution. Geochim. Cosmochim. Acta 41, 1097–1103.

Gwiazda, R.H., Broecker, W.S., 1994. The separate and combined effects of temperature, soil pCO_2, and organic acidity on silicate weathering in the soil environment: formulation of a model and results. Global Biogeochem. Cycles 8 (2), 141–155.

Helgeson, H.C., Murphy, W.M., Aagaard, P., 1984. Thermodynamic and kinetic constraints on reaction rates among minerals and aqueous solutions: II. Rate constants, effective surface area, and the hydrolysis of feldspar. Geochim. Cosmochim. Acta 58, 2405–2432.

Hering, J.G., 1995. Interaction of organic-matter with mineral surfaces — effects on geochemical processes at the mineral–water interface, Aquatic Chemistry. Adv. Chem. Ser., 95–119.

Hill, D.P., 1996. Earthquakes and carbon dioxide beneath Mammoth Mountain, California. Seismol. Res. Lett. 67, 8–15.

Hill, D.P., et al., 1990. The 1989 earthquake swarm beneath Mammoth Mountain, California: an initial look at the 4 May through 30 September activity. Bull. Seismol. Soc. Am. 80 (2), 325–339.

Knauss, K.G., Nguyen, S.N., Weed, H.C., 1993. Diopside dissolution kinetics as a function of pH, CO_2, temperature, and time. Geochim. Cosmochim. Acta 57, 285–294.

Kolka, R.K., Grigal, D.F., Nater, E.A., 1996. Forest soil mineral weathering rates: use of multiple approaches. Geoderma 73, 1–21.

Kraemer, S.M., Hering, J.G., 1997. Influence of solution saturation state on the kinetics of ligand-controlled dissolution of oxide phases. Geochim. Cosmochim. Acta 61 (14), 2855–2866.

Kraemer, S.M., Chiu, V.Q., Hering, J.G., 1998. Influence of pH and competitive adsorption on the kinetics of ligand-promoted dissolution of aluminum oxide. Environ. Sci. Technol. 32, 2876–2882.

Lagache, M., 1965. Contribution a l'etude de l'alteration des feldspaths, dans l'eau, entre 100 et 200 C, sous diverses pressions de CO_2, et application a la synthese des mineraux argileux. Bull. Soc. Fr. Mineral. Cristallogr. 88, 223–253.

Langmuir, D., 1997. Aqueous Environmental Geochemistry Prentice Hall, Upper Saddle River, NJ.

Malmstrom, M., Banwart, S., Lewenhagen, J., Duro, L., Bruno, J., 1996. The dissolution of biotite and chlorite at 25 °C in the near-neautral pH region. J. Contam. Hydrol. 21, 201–213.

Marshall, H.G., Walker, J.C.G., Kuhn, W.R., 1988. Long-term climate change and the geochemical cycle of carbon. J. Geophys. Res. 93, 791–801.

McCarty, D.K., Moore, J.N., Marcus, W.A., 1998. Mineralogy and trace element association in an acid mine drainage iron oxide precipitate; comparison of selective extractions. Appl. Geochem. 13, 165–176.

McGee, K.A., Gerlach, T.M., 1998. Annual cycle of magmatic CO_2 in a tree-kill soil at Mammoth Mountain, California: implications for soil acidification. Geology 26 (5), 463–466.

McKeague, J.A., Day, J.H., 1966. Dithionite- and oxalate-extractable Fe and Al as aids in differentiating various classes of soils. Can. J. Soil Sci. 46, 13–26.

Mehra, O.P., Jackson, M.L., 1960. Iron oxide removal from soils and clays by a dithionite-citrate system buffered with sodium bicarbonate. Clays Clay Miner. 7, 317–327.

Miller, C.D., 1985. Holocene eruptions at the Inyo volcanic chain, California: implications for possible eruptions in Long Valley caldera. Geology 13, 14–17.

Morel, F.M.M., Hering, J.G., 1993. Principles and Applications of Aquatic Chemistry Wiley, New York, 588 pp.

Ochs, M., 1996. Influence of humified and non-humified natural organic compounds on mineral dissolution. Chem. Geol. 132, 119–124.

Ochs, M., Brunner, I., Stumm, W., Cosovic, B., 1993. Effects of root exudates and humic substances on weathering kinetics. Water, Air, Soil Pollut. 68, 213–229.

Osthols, E., Malmstrom, M., 1995. Dissolution kinetics of ThO_2 in acids and carbonate media. Radiochim. Acta 68 (2), 113–119.

Pohlman, A.A., McColl, J.G., 1988. Soluble organics from forest litter and their role in metal dissolution. Soil Sci. Soc. Am. J. 52, 265–271.

Rahn, T.A., Fessenden, J.E., Wahlen, M., 1996. Flux chamber measurements of anomalous CO_2 emission from the flanks of Mammoth Mountain, California. Geophys. Res. Lett. 23 (14), 1861–1864.

Rogie, J.D., 2001. Personal communication, USGS, Menlo Park, CA.

Rogie, J.D., Kerrick, D.M., Sorey, M.L., Chiodini, G., Galloway, D.L., 2001. Dynamics of carbon dioxide emission at Mammoth Mountain, California. Earth Planet. Sci. Lett. 188, 535–541.

Schnoor, J.L., 1990. Kinetics of chemical weathering: a comparison of laboratory and field weathering rates. In: Stumm, W. (Ed.), Aquatic Chemical Kinetics: Reaction Rates of Processes in Natural Waters. Wiley, New York, pp. 475–504.

Seney, J.P., Gallegos, J.A., 1995. Soil Survey of Inyo National Forest, West Area, California. US Department of Agriculture, Forest Service, Washington, DC, 365 pp.

Shoji, S., Dahlgren, R., Nanzyo, M., 1993. Terminology, concepts and geographic distribution of volcanic ash soils. In: Shoji, S., Nanzyo, M., Dahlgren, R.A. (Eds.), Volcanic Ash Soils, Genesis, Properties and Utilization. Developments in Soil Science, vol. 21. Elsevier, Amsterdam, p. 288.

Sieh, K., 2000. Personal communication. Professor of Geology, California Institute of Technology, Pasadena, CA.

Sorey, M.L., et al., 1996. Invisible CO_2 Gas Killing Trees at Mammoth Mountain, California US Geological Survey, Menlo Park, CA.

Sorey, M.L., et al., 1998. Carbon dioxide and helium emissions from a reservoir of magmatic gas beneath Mammoth Mountain, California. J. Geophys. Res. 103 (B7), 15303–15323.

Sparks, D.L., 1989. Rates of Chemical Weathering, Kinetcis of Soil Chemical Processes. Academic Press, San Diego, pp. 146–162.

Sposito, G., 1984. The Surface Chemistry of Soils Oxford Univ. Press, New York, 234 pp.

Stephens, J.C., 2002. Response of Soil Mineral Weathering to Elevated CO_2 Concentrations, California Institute of Technology, Pasadena, CA, in preparation.

Stumm, W., 1992. Chemistry of the Solid–Water Interface: Processes at the Mineral–Water and Particle–Water Interface in Natural Systems. Wiley, New York.

Sverdrup, H.U., 1990. The Kinetics of Base Cation Release Due to Chemical Weathering. Lund Univ. Press, 246 pp.

Sverdrup, H., Warfvinge, P., 1993. Calculating field weathering rates using a mechanistic geochemical model PROFILE. Appl. Geochem. 8, 273–283.

Velbel, M.A., 1989. Effect of chemical affinity on feldspar hydrolysis rates in two natural weathering systems. Chem. Geol. 78, 245–253.

Volk, T., 1987. Feedback between weathering and atmospheric CO_2 over the last 100 million years. Am. J. Sci. 287, 763–779.

White, A.F., 1995. Chemical weathering rates of silicate minerals in soils. In: White, A.F., Brantley, S.L. (Eds.), Chemical Weathering Rates of Silicate Minerals. Mineralogical Society of America, Washington, DC, pp. 407–463.

Whittig, L.D., Allardice, W.R., 1986. X-ray diffraction techniques. In: Klute, A. (Ed.), Methods of Soil Analysis: Part 1. ASA and SSSA, Madison, WI, pp. 331–362.

Wogelius, R.A., Walther, J.V., 1991. Olivine dissolution at 25 °C: effects of pH, CO_2, and organic acids. Geochim. Cosmochim. Acta 55 (4), 943–954.

Zabowski, D., Sletten, R.S., 1991. Carbon dioxide degassing effects on the pH of Spodosol soil solutions. Soil Sci. Soc. Am. J. 55, 1456–1461.